Rapid changes in flagellar rotation induced by external electric pulses

Nobunori Kami-ike,* Seishi Kudo,‡ and Hirokazu Hotani*§

ERATO (Exploratory Research for Advanced Technology), Molecular Dynamic Assembly Project, *15 Morimoto-cho Shimogamo, Sakyo-ku, Kyoto 606; ‡5-9-5 Tokodai, Tsukuba 300-26; and §Department of Biosciences, Teikyo University, Toyosatodai, Utsunomiya 320, Japan

ABSTRACT The bacterial flagellar motor is the only molecular rotary machine found in living organisms, converting the protonmotive force, i.e., the membrane voltage and proton gradients across the cell membrane, into the mechanical force of rotation (torque). We have developed a method for holding a bacterial cell at the tip of a glass micropipette and applying electric pulses through the micropipette. This method has enabled us to observe the dynamical responses of flagellar rotation to electric pulses that change the membrane voltage transiently and repeatedly. We have observed that acceleration and deceleration of motor rotation are induced by application of these electric pulses. The change in the rotation rate occurred within 5 ms after pulse application.

INTRODUCTION

Bacteria swim by the rotation of their flagella (Berg and Anderson, 1973; Silverman and Simon, 1974), each of which is driven by a motor embedded in the cell surface. The motor is a molecular machine made up of proteins and is powered by the protonmotive force across the cell membrane (Manson et al., 1977; Matsuura et al., 1977; Glagolev and Skulachev, 1978). The mechanism of torque generation is not yet known, partly because of the experimental difficulties in measuring the dynamic input-to-output characteristics of an individual motor.

The protonmotive force, i.e., the membrane voltage and proton gradients across the cell membrane, has been manipulated previously by various methods, such as the addition of ionophores or lipophilic cations to the medium, and subsequent changes in motor rotation rate measured in tethered cells or by swimming speed measurements (Manson et al., 1977; Matsuura et al., 1977; Glagolev and Skulachev, 1978; Shioi et al., 1980; Manson et al., 1980; Khan et al., 1990). The changes in the protonmotive force, however, have been rather slow because diffusion of the reagents is rate limiting. Caged protons have been used to generate transient increases in the proton gradient and the time required for changes in the rotation rate of tethered cells found to be in the range of 15–150 ms (Shimada and Berg, 1987). However, the reverse experiment, transient decreases of the proton gradient, has not yet been possible. The transient and reversible control of the membrane voltage of a single bacterium by electrophysiological methods has been considered impractical, because the size of a bacterial cell body is too small to allow insertion of a micropipette. Furthermore, high speed rotation of a single flagellum has been difficult to measure, because the diameter of the flagellar filament is very small ($\sim$24 nm) (Trachtenberg and DeRosier, 1987; Namba et al., 1989).

Recently, Kudo et al. (1990) have developed a new method, laser dark-field microscopy, for the measurement of the high speed rotation of single flagella. Here, we have developed a method to hold a single bacterial cell body at the tip of a glass micropipette, so that we can transiently change the membrane voltage by applying electric pulses through the micropipette and simultaneously measure the rotation rate of a single flagellum by the laser dark-field microscopy. We have found that acceleration and deceleration of rotation are induced by hyperpolarization and depolarization, respectively, of the membrane containing the motor. The changes in rotation rate occurred within $\sim$5 ms after the pulse application. These results clearly demonstrate that the flagellar motor can be driven by membrane voltage alone, which is one of the components of protonmotive force.

This is a direct demonstration that rotation of the flagellar motor can be controlled by an external electric field. It also provides a method to measure the voltage-dependent kinetic properties of flagellar motor function, which in turn should help us understand the elementary processes of torque generation.

MATERIALS AND METHODS

Materials

A *che*-deletion strain of *Salmonella typhimurium*, which lacks all six *che* genes (*che*AWRBYZ), SJW3076 (Magariyama et al., 1990), was supplied by Dr. S. Yamaguchi (Meiji University, Japan). Cells were grown to late-log phase at room temperature in Luria broth medium (pH 6.9).

Setup of experimental apparatus

Fig. 1 *a* shows the experimental apparatus. The inner diameter of the tip of the aspirating micropipette is $\sim$1 μm, and that of the reference

0006-3495/91/12/1350/06 $2.00

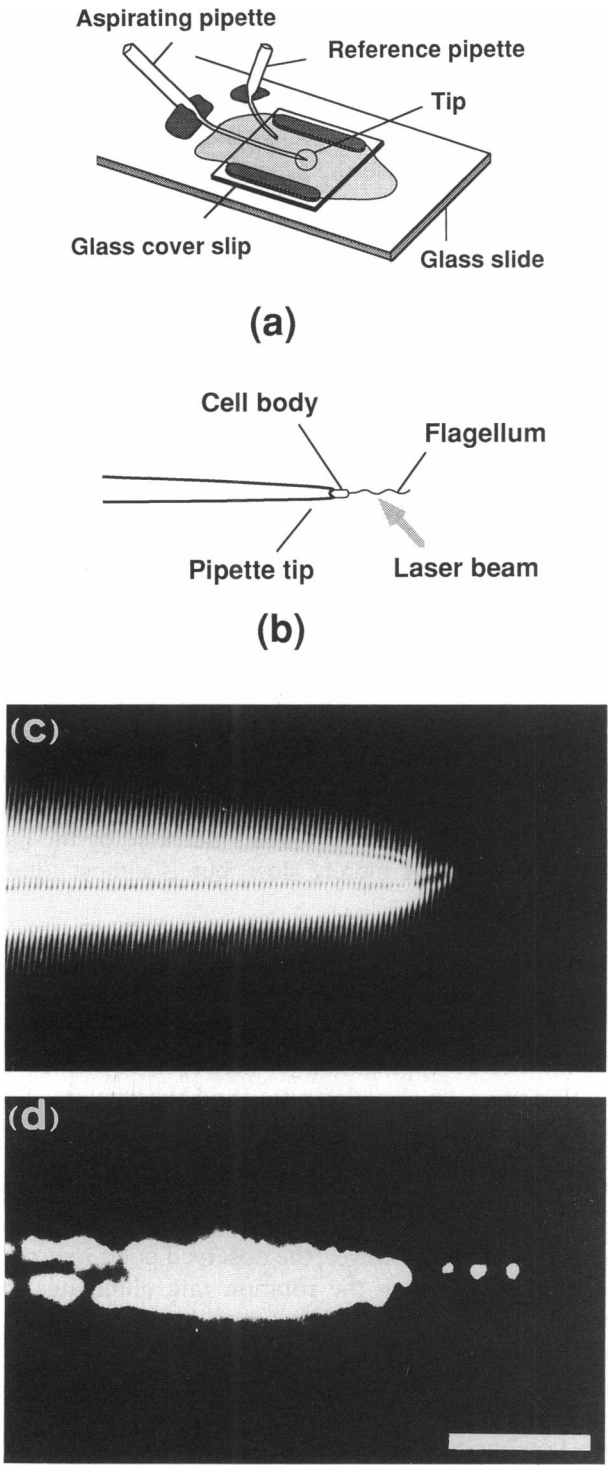

FIGURE 1 Schematic drawing of the experimental setup and micrographs of the micropipette tip and an aspirated bacterium. (*a*) Experimental apparatus. (*b*) Illustration of bacterium, micropipette tip, and direction of laser illumination. (*c*) A phase contrast micrograph of a bacterium held at the tip of the micropipette. (*d*) A laser dark-field micrograph of the same bacterium and the micropipette, showing a flagellum as a series of bright spots. Bar, 10 μm.

micropipette is ~50 μm. To minimize loss of the applied voltage, the reference micropipette has a very low resistance in comparison with the aspirating micropipette. These two micropipettes are fixed to a glass slide with wax, a cover slip is placed over them and fixed with Vaseline, then the gap between the glass slide and the cover slip is filled with standard medium (fresh Luria broth medium, pH 6.9). 5 μl of the bacterial culture is then introduced into the gap between the glass slide and the cover slip. Ag/AgCl electrodes are electrically connected directly to the medium in the aspirating pipette and through a salt bridge in the reference pipette. The aspirating pipette and the Ag/AgCl electrode are attached to a patch clamp pipette holder. The voltage pulse through the aspirating micropipette is applied by a high voltage operational amplifier (model 1032; Teledyne, Dedham, MA) and the resulting current is detected by the reference electrode.

Experimental procedures

An actively swimming bacterial cell was caught at the tip of a micropipette by simply aspirating the medium containing bacterial cells. One or more flagellar filaments were usually seen rotating freely in the medium outside of the micropipette. A single rotating flagellum was then observed by laser dark-field microscopy described by Kudo et al. (1990). Fig. 1 *b* shows schematically an aspirated bacterium, micropipette tip, and the direction of laser illumination. Fig. 1, *c* and *d* show a phase contrast and a laser dark-field micrograph, respectively, of the same bacterium held at the tip of the micropipette. In Fig. 1 *c*, the phase contrast image was recorded with a video camera. Fig. 1 *d* shows the flagellum as a series of bright spots and the micropipette as a bright rod (*left side*). The spots move along the helical axis with flagellar rotation. The dark-field image of a single flagellum illuminated by a laser beam was focused on a mirror with a narrow slit so that the light passing through the slit was detected with a photomultiplier tube (model R453; Hamamatsu Photonics, Hamamatsu, Japan). The rotation of the flagellum was measured as the cyclic intensity change of the light coming through the slit. One cycle of the light intensity change corresponds to one cycle of rotation of the flagellum. The rotation rates (rps) were determined from the intervals between the peaks. During the experiment, the standard medium was constantly perfused (from left to right in Figs. 1, *b–d*) in order to stabilize the orientation of the flagellum. The flow of medium (~ 10 μm/s) had very little effect on the rotation rate (< 1%). Experiments were performed at room temperature. Light intensity, applied voltage, and micropipette current were simultaneously recorded on a digital data recorder (RD-101T; TEAC, Tokyo). The recorded data were analyzed by personal computer systems after the analogue-to-digital conversion.

Note that when a voltage pulse is applied between the aspirating and reference micropipettes, a negative pulse generates an inward current through the membrane outside of the micropipette tip, hyperpolarizing this portion of the membrane (Fig. 2). In contrast, a positive pulse

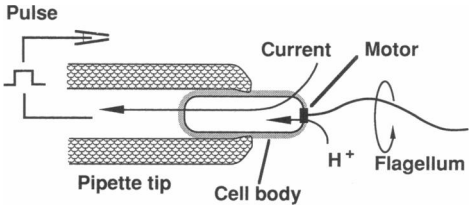

FIGURE 2 Schematic drawing of the tip of the aspirating micropipette and a bacterial cell body attached to it illustrating the current flow induced by a negative (hyperpolarizing) pulse.

induces depolarization of the membrane outside the micropipette tip.

RESULTS

Acceleration and deceleration of flagellar rotation by external electric pulses

Fig. 3, *a* and *b* show typical examples of temporal acceleration of rotation induced by hyperpolarizing pulses. A pulse of −2.4 V with 0.3-s duration induced a rapid increase in the rotation rate from 28 ± 2 to 38 ± 2 rps and the rate rapidly recovered to 24 ± 4 rps upon termination of the pulse (Fig. 3 *a*). A pulse of −5.9 V induced a rapid increase in the rotation rate from 47 ± 3 to 73 ± 6 rps and the rate recovered to 51 ± 4 rps (Fig. 3 *b*). Fig. 3 *c* and *d* shows typical examples of the deceleration of the rotation induced by depolarizing pulses. A 1.7-V pulse of 0.3-s duration induced a rapid decrease in the rotation rate from 105 ± 6 to 76 ± 8 rps and the rotation rate recovered to 101 ± 7 rps upon termination of the pulse (Fig. 3 *c*). A 7.1-V pulse induced a rapid decrease in the rotation rate from 105 ± 10 to 21 ± 12 rps and the rotation rate initially recovered to 78 ± 5 rps (Fig. 3 *d*). In this case, the deceleration occurred within 5 ms, but the initial recovery had an ~80-ms delay. The rotation rate then further increased gradually for a few seconds to reach its original level. That is, the recovery was in two steps, a first rapid step lasting a few milliseconds resulting in ~75% recovery and a second slow step lasting a few seconds to achieve 100% recovery. In the case of Fig. 3 *d*, where the rotation was irregular and the intensity record was noisy, the peaks were distinguished from noise by their intensities (>0.6). The light intensity in Fig. 3, *a–d* is given in arbitrary units (au).

In most cases only a short delay time (<5 ms) was observed for the rate changes at the beginning and termination of a pulse, as in Fig. 3 *a–c*. However, when depolarizing pulses greater than ~2 V were applied, the decelerated rotation was irregular and was prolonged for 92 ± 14 ms (n = 10) after the termination of the pulses as shown in Fig. 3 *d*, and then recovery occurred in two steps: an initial, rapid step, lasting a few milliseconds; followed by a slow step lasting a few seconds, which achieved complete recovery.

Relationship between the rotation rate and the applied voltage

Fig. 4 shows relationships between the flagellar rotation rate and the amplitude of the applied pulse. The positive and negative values on abscissa are the depolarizing and hyperpolarizing voltages, respectively. Open circles, closed circles, and triangles represent the data from three different cells which were repeatedly pulsed. The values of rotation rate at 0 V were averaged over 0.3 s immediately before each pulse application. Each voltage pulse data point is also the average rotation rate over a 0.3-s time period. The standard deviations of the rotation rates at 0 V were 7% (n = 17, *open circle*), 20% (n = 28, *closed circle*), and 19% (n = 16, *triangle*), indicating that the motor maintained its characteristics fairly well over the course of each experiment (~10 min).

Transitions of the rotation rate by electric pulses

The transitions in the rotation rate caused by the hyperpolarizing and depolarizing pulses are shown on an expanded time scale in Fig. 5, *a* and *b*. In both cases, the rotation rates changed almost immediately after the application of the pulse. The delay times are estimated to be 5 ms or less from the light intensity profiles at the transition. For example, in Fig. 5 *b*, the depolarizing pulse was applied at the top of the peak indicated by an arrow. The rotation rate, however, remained constant for a half cycle of rotation and then decelerated (the intensity changes from the peak to the next trough took ~5 ms). Note that at the plateau indicated by the bar, the rotation is not merely slow, but is almost totally suppressed.

DISCUSSION

The most direct explanation for the observed changes in rotation rate is the depolarization and hyperpolarization of the membrane which are induced by the voltage pulses though the aspirating micropipette. Other possible causes for the change in rotation rate include either heat generation or electrophoretic water flow at the micropipette tip. However, the observed polar nature of the voltage effect on the rotation rate eliminates the former possibility. We have observed that large pulses induce a water flow through the micropipette tip in the absence of a bacterial cell. This flow, however, would rotate a helical structure such as the flagellum in a direction opposite to that which we observed; for example, a hyperpolarizing pulse induces an inward flow of medium, but because of the flagellum's helical geometry, an inward flow of medium would decrease the rate of rotation, not increase it, as was observed. Therefore, the latter possibility can also be ruled out. We conclude that change in membrane potential is indeed responsible for the change in rotation rate.

Much higher voltages than those used in ordinary

electrophysiological experiments were necessary to induce significant changes in the flagellar rotation rate. This is because the electrical resistance of the seal between the cell surface and the glass pipette is low and, therefore, most of the applied current leaks through the seal. The average resistance of aspirating micropipettes was 0.8 ± 0.7 gigaOhm (n = 10), when no bacterium was trapped at the tip. Blocking the micropipette with a

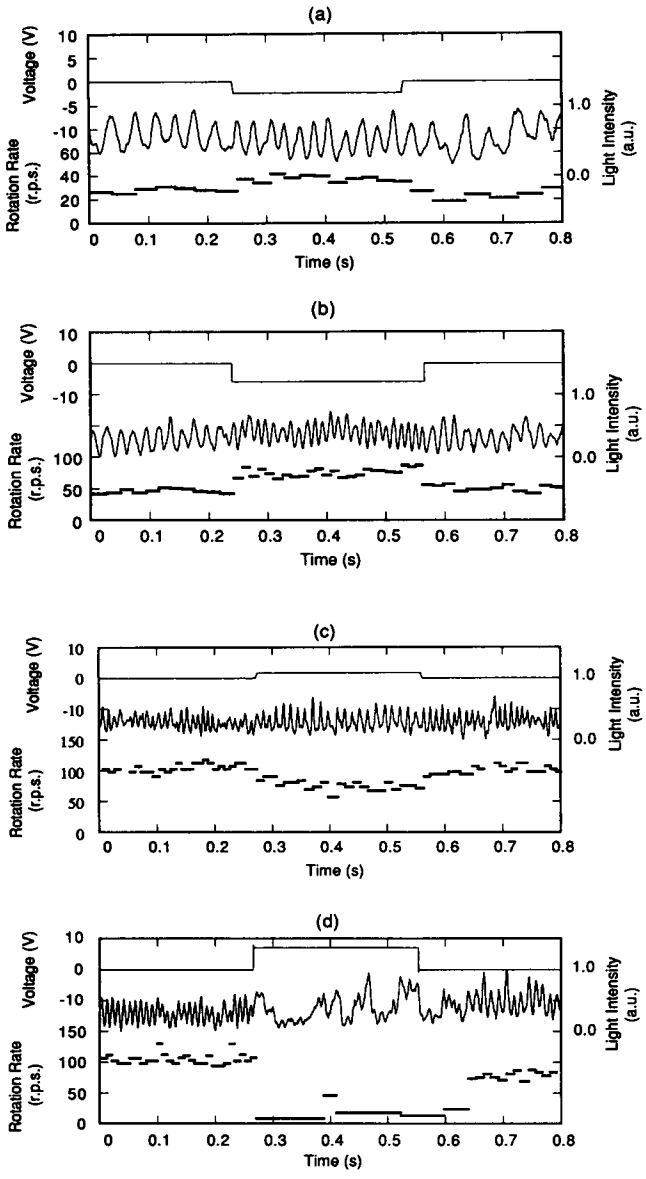

FIGURE 3 Rotation rate changes induced by various amplitude of voltage pulses. Upper, middle, and lower traces are the applied voltage, light intensity, and rotation rate (see text for details), respectively. *a* and *b* are typical examples of acceleration of the rotation induced by hyperpolarizing pulses (*a*, −2.4 V; *b*, −5.9 V). *c* and *d* are typical examples of the deceleration of the rotation induced by depolarizing pulses (*c*, +1.7 V; *d*, +7.1 V).

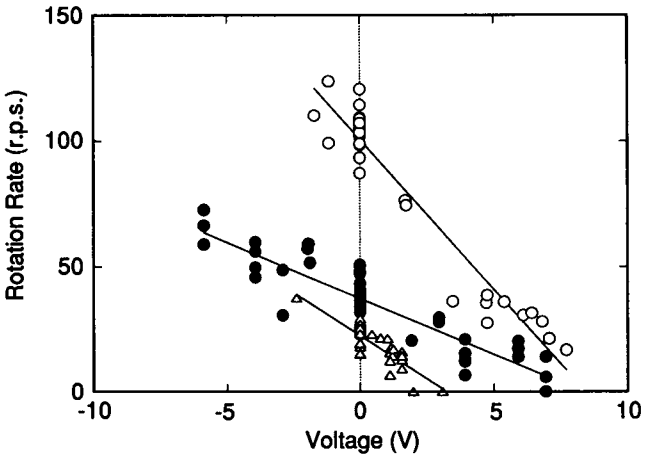

FIGURE 4 Relationship between flagellar rotation rate and amplitude of the applied pulse. The positive and negative values on the abscissa are the depolarizing and hyperpolarizing voltages, respectively. Each symbol (*open circles, closed circles,* and *triangles*) represents the data from a single cell which was repeatedly pulsed. The solid lines were obtained by linear regression analysis of each data set.

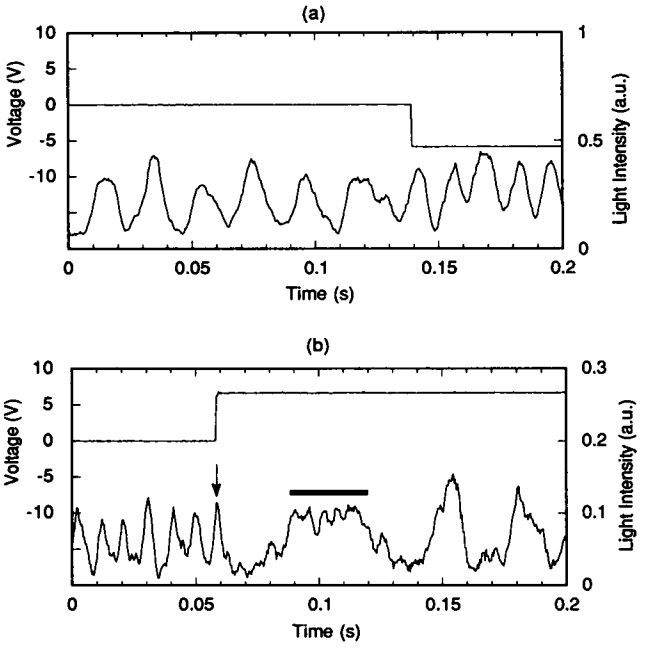

FIGURE 5 Transition in rotation rate caused by depolarizing and hyperpolarizing pulses shown on an expanded time scale. (*a*) A transition by a hyperpolarizing pulse (−5.9 V). (*b*) A transition by a depolarizing pulse (+6.7 V). Upper and lower traces are the applied voltage and light intensity. In *b*, the arrow indicates the onset of the applied voltage, and the black bar indicates a period of almost total cessation of rotation.

bacterial cell body induced only a 21 ± 20% (n = 10) increase in the resistance. The seal has a low resistance probably because either the cell wall has low resistivity or the contact between the cell surface and the glass micropipette is loose. In a Gram-negative bacterium, such as *S. typhimurium,* the cell surface consists of an outer membrane, a peptidoglycan cell wall, a periplasmic space, and a cytoplasmic membrane (reviewed by Nikaido and Vaara, 1987; Oliver, 1987). The outer membrane, which has large pores, is considered to have very low resistivity compared with the cytoplasmic membrane.

Application of a hyperpolarizing pulse caused a rapid increase in the rotation rate, and a depolarizing pulse decreased the rotation rate. In both cases, the rate normally recovered quickly upon termination of the pulse. However, when a large depolarizing pulse was applied, the decelerated rotation was irregular and was prolonged after the termination of the pulse. Irregular rotation at low protonmotive force has also been observed in tethered cells under high load conditions (Khan et al., 1985). This irregularity and delay may relate to some unknown characteristics of the motor. They may originate from thermal fluctuations and/or the stepwise property of torque generation of the motor.

The change in rotation rate was roughly proportional to the pulse amplitude in the observed voltage range, but the slopes showed wide variation. Also, the intersections with the abscissa were variable, although they coincide for two of the cases shown in Fig. 4 (*open* and *closed circles*). Quantitative determination of the relationship between rotation rate and membrane voltage using our method is difficult, because the actual change in the membrane voltage depends on the resistance distribution around the micropipette and bacterial cell body and could not be directly monitored. However, this system is good enough for the qualitative analysis of the dynamic properties of single bacterial flagellar motors.

In both cases shown in Fig. 5, the rotation rate changed within 5 ms after the application of the pulse. The time constant of the membrane voltage change of bacterial cells is estimated from its capacitance and resistance (Felle et al., 1978) to be 2 ms. This suggests that the actual response time of the motor is shorter than 3 ms. This response time is a fifth or less of that obtained in the experiments using caged protons (Shimada and Berg, 1987). The difference in response times derived using the two methods may reflect a delay arising from the diffusion of the (released) caged protons or buffering effects in the cell wall and periplasmic space.

Input perturbation and detection of the resulting output change is generally one of the most powerful ways available to examine an unknown mechanism in any system. The dynamic and static response of single flagellar motors to rapid perturbation of the input can be investigated by applying an external electric field as described above. The obtained relationship between input and output of the motor should allow us to analyze voltage-dependent kinetics in a way similar to that which has been used with the *Chara* proton pump (Kishimoto et al., 1984; Kami-ike et al., 1986) and to evaluate the various kinetic models of the motor (Oosawa and Hayashi, 1983; Läuger, 1988; Meister et al., 1989). This study, therefore, opens up a new way to examine the energy transduction mechanism of the flagellar motor. This system is unique in the sense that such dynamical perturbations of input are difficult to apply to other systems of chemomechanical coupling such as the one used in muscle or cilia, because these use ATP as an energy input (not membrane potential), and the diffusion of ATP is the rate-limiting step in these systems.

We thank F. Oosawa, Y. Imae, H. Nakayama, K. Namba, and S.-I. Aizawa for support and discussions throughout this work, S. Yamaguchi for the bacterial strain, S. Hayashi for technical help, and S. A. Salehi, T. Ikeda, T. J. Itoh, M. Seville, and C. J. Jones for critically reading the manuscript.

Received for publication 13 May 1991 and in final form 5 August 1991.

REFERENCES

Berg, H. C., and R. A. Anderson. 1973. Bacteria swim by rotating their flagellar filaments. *Nature (Lond.)*. 245:380–382.

Felle, H., D. L. Stetson, W. S. Long, and C. L. Slayman. 1978. Direct measurement of membrane potential and resistance in giant cells of *Escherichia coli. In* Frontiers of Biological Energetics. P. L. Dutton, J. S. Leigh, and A. Scarpa, editors. Academic Press, New York 2:1399–1407.

Glagolev, A. N., and V. P. Skulachev. 1978. The proton pump is a molecular engine of motile bacteria. *Nature (Lond.)*. 272:280–282.

Kami-ike, N., T. Ohkawa, U. Kishimoto, and Y. Takeuchi. 1986. A kinetic analysis of the electrogenic pump of *Chara corallina:* IV. Temperature dependence of the pump activity. *J. Membr. Biol.* 94:163–171.

Khan, S., M. Meister, and H. C. Berg. 1985. Constraints on flagellar rotation. *J. Mol. Biol.* 184:645–656.

Khan, S., M. Dapice, and I. Humayun. 1990. Energy transduction in the bacterial flagellar motor. Effects of load and pH. *Biophys. J.* 57:779–796.

Kishimoto, U., N. Kami-ike, Y. Takeuchi, and T. Ohkawa. 1984. A kinetic analysis of the electrogenic pump of *Chara corallina:* I. Inhibition of the pump by DCCD. *J. Membr. Biol.* 80:175–183.

Kudo, S., Y. Magariyama, and S.-I. Aizawa. 1990. Abrupt changes in flagellar rotation observed by laser dark-field microscopy. *Nature (Lond.)*. 346:677–680.

Läuger, P. 1988. Torque and rotation rate of the flagellar motor. *Biophys. J.* 53:53–65.

Magariyama, Y., S. Yamaguchi, S.-I. Aizawa. 1990. Genetic and behavioral analysis of flagellar switch mutants of *Salmonella typhimurium. J. Bacteriol.* 172:4359–4369.

Manson, M. D., P. M. Tedesco, H. C. Berg, F. M. Harold, and C. van der Drift. 1977. A protonmotive force drives bacterial flagella. *Proc. Natl. Acad. Sci. USA.* 74:3060–3064.

Manson, M. D., P. M. Tedesco, and H. C. Berg. 1980. Energetics of flagellar rotation in bacteria. *J. Mol. Biol.* 138:541–561.

Matsuura, S., J. Shioi, and Y. Imae. 1977. Motility in *Bacillus subtilis* driven by an artificial protonmotive force. *FEBS Lett.* 82:187–190.

Meister, M., S. R. Caplan, and H. C. Berg. 1989. Dynamics of a tightly coupled mechanism for flagellar rotation. *Biophys. J.* 55:905–914.

Namba, K., I. Yamashita, and F. Vonderviszt. 1989. Structure of the core and central channel of bacterial flagella. *Nature* (*Lond.*). 342:648–654.

Nikaido, H., and M. Vaara. 1987. Outer membrane. *In Escherichia coli* and *Salmonella typhimurium:* Cellular and Molecular Biology. F. C. Neidhardt, J. L. Ingraham, K. Brooks Low, B. Magasanik, and M. Schaechter, editors. American Society for Microbiology, Washington, DC. 1:7–22.

Oliver, B. D. 1987. Periplasm and protein secretion. *In Escherichia coli* and *Salmonella typhimurium:* Cellular and Molecular Biology. F. C. Neidhardt, J. L. Ingraham, K. Brooks Low, B. Magasanik, and M. Schaechter, editors. American Society for Microbiology, Washington, DC. 1:56–69.

Oosawa, F., and S. Hayashi. 1983. Coupling between flagellar motor rotation and proton flux in bacteria. *J. Phys. Soc. Japan.* 52:4019–4028.

Shimada, K., and H. C. Berg. 1987. Response of the flagellar rotary motor to abrupt changes in extracellular pH. *J. Mol. Biol.* 193:585–589.

Shioi, J., S. Matsuura, and Y. Imae. 1980. Quantitative measurements of proton motive force and motility in *Bacillus subtilis. J. Bacteriol.* 144:891–897.

Silverman, M., and M. Simon. 1974. Flagellar rotation and the mechanisms of bacterial motility. *Nature* (*Lond.*). 249:73–74.

Trachtenberg, S., and D. J. DeRosier. 1987. Three-dimensional structure of the frozen-hydrated flagellar filament: the left-handed filament of *Salmonella typhimurium. J. Mol. Biol.* 195:581–601.